Flexible Electronics Applications of Ge-rich and Se-Substituted Phase-change Materials in Non-volatile Memories

Joe Pady, Julio Costa, Catherine Ramsdale, Feras Alkhalil, Aimee Nevill, Monica F. Craciun and C. David Wright**

J. Pady, M. F. Craciun, C. D. Wright
Department of Engineering, University of Exeter, EX4 4QF, UK
E-mail: david.wright@exeter.ac.uk, jp551@exeter.ac.uk

J. Costa, C. Ramsdale, F. Alkhalil, A. Nevill
PragmatIC Semiconductor, Cambridge, CB4 0WH, UK

Keywords: Ge-rich GST, electrical properties, flexible memory

Abstract: Flexible electronics which are easy to manufacture and integrate into everyday items require suitable memory technology that can function on flexible surfaces. Here the properties of Ge-rich GeSbTe (GST) and Se-substituted GeSbSeTe (GSST) phase-change alloys are investigated for application as non-volatile write-once and rewritable memories in flexible electronics. These materials have a higher crystallization temperature than the archetypal composition of $Ge_2Sb_2Te_5$, hence better data retention properties. Moreover, their high crystallization temperature provides for a particularly straightforward implementation of a write-once memory configuration. Material properties of Ge-rich GST and GSST are measured as a function of temperature using 4-point probe electrical testing, Raman spectroscopy and X-ray diffraction. Following this, the switching of flexible memory devices is investigated through both simulation and experiment. More specifically, crossbar memory devices fabricated using Ge-rich GST were experimentally fabricated and tested, while the operation of GSST pore cell structures suitable for flexible memory applications was demonstrated through simulation.

1. Introduction

To help realise wide scale implementation of Internet of things[1] (IoT) technology, flexible integrated circuits are required to expand the range of everyday items that can have smart capabilities. An important requirement of these circuits is to have functioning data storage on flexible substrates; to realise this, memory devices that can be fabricated on flexible surfaces and remain functional on these surfaces are a key requirement. Some of the applications of flexible IoT technology are medical and sports tracking, environmental monitoring and radio-frequency identification (RFID) technology,[2,3] where objects are embedded with tags which can transmit unique information using radio frequencies. Phase-change memory (PCM) is an emerging non-volatile memory technology. As well as its potential applications for highly scalable[4] and high performance[5] memories, it also shows promise for use in flexible memories,[6] including low-cost and flexible integrated circuits (FlexICs) for non-volatile data and code storage.[7] Some potential compositions for use in flexible PCMs are Ge-rich GeSbTe (GST) alloys. Germanium enrichment causes a higher crystallization temperature than the archetypal composition of $Ge_2Sb_2Te_5$ (GST-225),[8,9] leading to better data retention properties.[10] A high crystallization temperature also enables the amorphous state to withstand a wider range of high temperature manufacturing processes, in turn making the development of a simple write-once memory, in which a single switch from amorphous to crystalline state is used, more straightforward. However, for re-writable applications, Ge-rich GST compositions have the potential to undergo unwanted recrystallization in the amorphization operation. This is because low-cost flexible electronics systems are often limited to using much longer pulse durations compared to conventional memory cells. Therefore, materials like GST alloys – which are optimised for rapid switching – may recrystallize too readily upon cooling. To overcome this challenge selenium substituted GSST compositions are suggested. These materials have a significantly reduced crystallization speed – so potentially preventing unwanted crystallization during amorphization - whilst still offering a high crystallization temperature.[11]

2. Material Characterization

Here, three compositions are explored for potential application as phase-change memories to be used in flexible electronics: these are the germanium rich compounds $Ge_7Sb_2Te_5$ (GST-725)[12] and $Ge_8Sb_2Te_5$ (GST-825), as well as $Ge_2Sb_2Se_4Te$ (GST-2241)[13] where tellurium has been substituted by selenium. To assess these materials' performance for flexible electronics applications their temperature dependent crystallization properties were

investigated through measurements of electrical resistivity as a function of temperature, as well as by obtaining Raman and X-ray diffraction (XRD) spectra. To facilitate this, 100 nm thin films of the three compositions were deposited via magnetron sputtering (Nordiko 2000) onto Si/SiO_2 substrates with a 50 nm oxide layer. Then the samples were heated on a programmable hotplate (EchoTherm HP60A-2) in the range of room temperature to 350°C with a ramp of 7.5°Cmin^{-1}, and a 4-point probe was used to measure in-situ resistance as a function of temperature (Keithley 2400). **Figure 1** shows the measured resistivity for each material, as well as the archetypal GST-225 material for comparison. The dramatic reductions in electrical resistivity indicate the onset of crystallization as the high resistance amorphous phase is switching to the low resistance crystalline phase. Here we see both Ge-rich GST compounds and GSST-2241 have a significantly higher crystallization temperature than GST-225. Amorphous resistivity levels are retained for temperatures up to ~210°C for Ge-rich GST and to ~280°C for GSST-2241. This is similar to previously published values for these materials.[9,14]

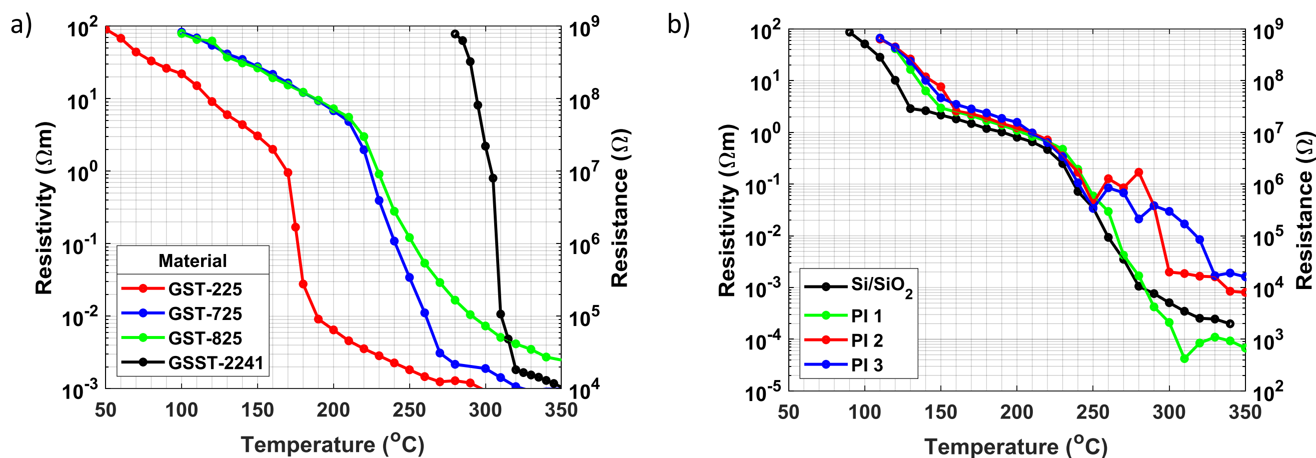

Figure 1. a) In situ measurements of the electrical resistivity and resistance of GST-225, GST-725, GST-825 and GSST-2241 on Si/SiO_2 substrates as a function of temperature. Rapid decrease in resistivity indicates phase-change from the amorphous to crystalline state. b) In situ measurements of the electrical resistivity and resistance, as a function of temperature, of three GST-725 samples deposited on polyimide substrates (PI 1, 2 & 3). Results for a sample deposited on Si/SiO_2 included for comparison.

In addition to depositing films on Si/SiO_2 substrates, 100 nm thick GST-725 layers were deposited on polyimide (PI) substrates mounted on glass. PI is a flexible polymer that is commonly used as a substrate for flexible electronics. In Figure 1 in-situ measurements of electrical resistivity of GST-725 on PI indicate that crystallization occurs at around the same temperatures of ~280°C as it does for the conventional, non-flexible silicon-based substrates used previously, indicating that the use of a flexible substrate does not have a significant effect on the crystallization temperature (at least of GST-725). We note that there is some variation in the measured resistivity for PI samples 2 and 3 above 250 ^{o}C. The reasons for this are not entirely clear, but could be due to minor deformation of the PI films at elevated temperatures causing a poorer quality contact between the probes and material surface.

To obtain further insights into material processes occurring upon crystallization of Ge-rich GST materials, 500 nm thick films of GST-725 were deposited on Si/SiO_2 substrates and subsequently annealed for 30 minutes at 300°C and 400°C in a (JIPELEC Jetfirst 200) rapid thermal processor. Next, Raman (Horiba XploRA Nano) spectra were obtained, followed by XRD (Bruker D8 Advance) patterns using X-ray wavelength 0.154 nm, with exemplar results being shown in **Figure 2**. The data at 300°C indicate that a GST component of the Ge-rich GST has crystallized. This agrees with the previously reported Ge-rich GST crystallization mechanism which involves Ge segregation followed by GST crystallization.[15] The exact stoichiometry of this GST component is not known, as GST compositions which fall along the GeTe-Sb_2Te_3 pseudo-binary line have almost identical lattice parameters and so can lead to the same XRD peaks.[16] The data at 400°C indicates that crystallization of segregated Ge clusters has started to occur as extra peaks corresponding to Ge appear in both the XRD patterns and Raman spectra. This again matches the previously reported temperature for Ge segregated cluster crystallization in Ge-rich phase-change materials of above 380°C.[17]

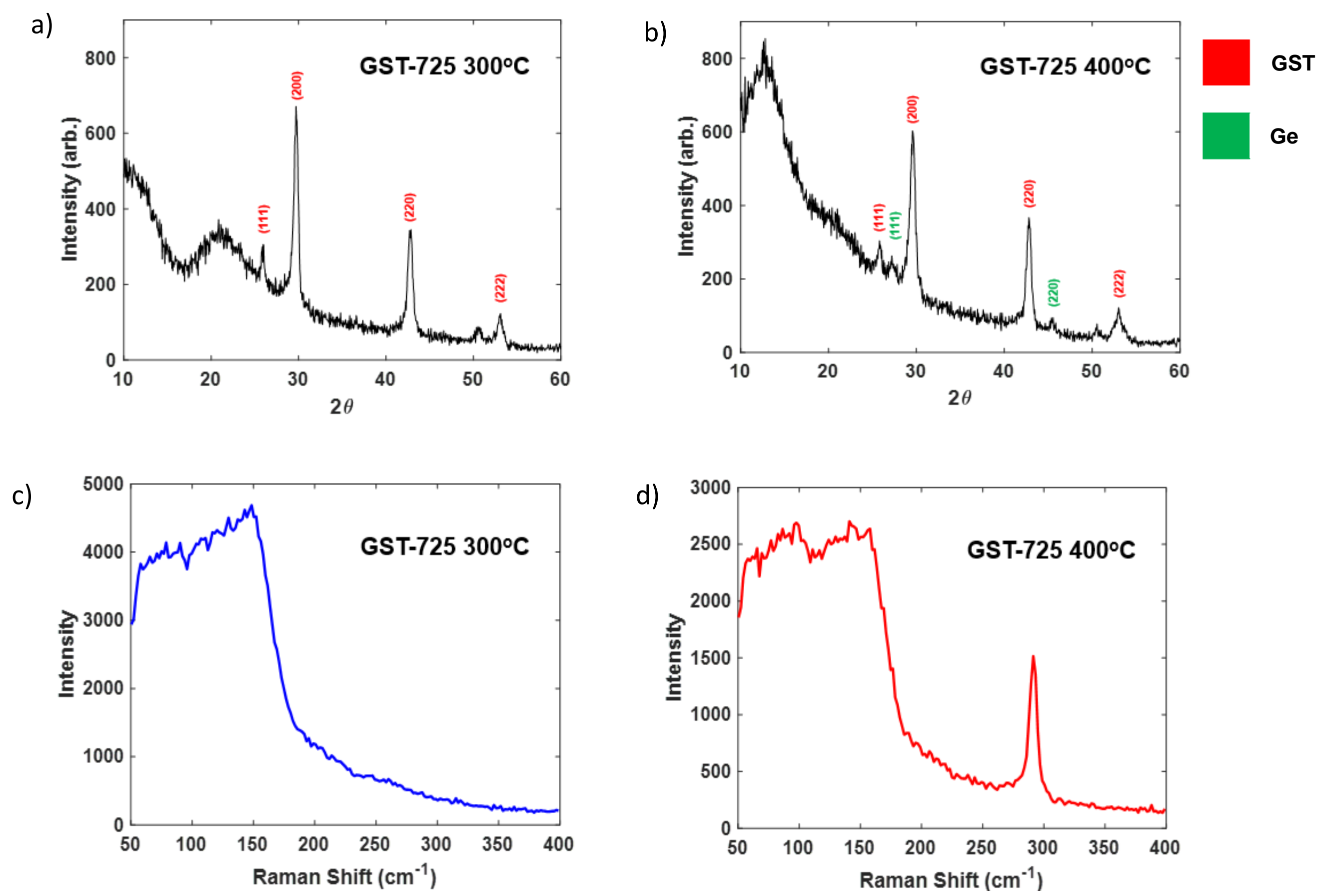

Figure 2. XRD pattern of GST-725 annealed for 30 minutes at a) 300°C and b) 400°C. The extra peaks appearing in the 400°C pattern indicate that crystallization of segregated Ge clusters has occurred. Raman spectra of GST-725 annealed for 30 minutes at c) 300°C and d) 400°C. The peak appearing at ~290 cm^{-1} also indicates Ge segregation and crystallization.

3. Crossbar Memory Devices

To demonstrate the basic functioning of memory devices made using Ge-rich GST, crossbar devices[18] were fabricated using GST-725 on Si/SiO_2 substrates. Electrodes were patterned using electron beam lithography (Nanobeam nB4) and materials deposited by magnetron sputtering. The bottom electrode consisted of 5 nm/5 nm of Ti/Pt, the GST-725 thickness was 30 nm and the top electrode was 30 nm of Pt. The cross region was 1 µm x 1 µm in size and the electrodes were connected to electrical contact pads to allow for easy connection to a probe system. The experimental switching of the Ge-rich crossbar cells was carried out using an I-V tester (Keithley 2400). **Figure 3** shows a microscope image of the cross region of the fabricated devices, as well as the I-V curve obtained starting from the as-deposited,

amorphous phase of the device. Characteristic threshold switching from the amorphous to crystalline phase was observed, along with a resistance contrast of ~100.

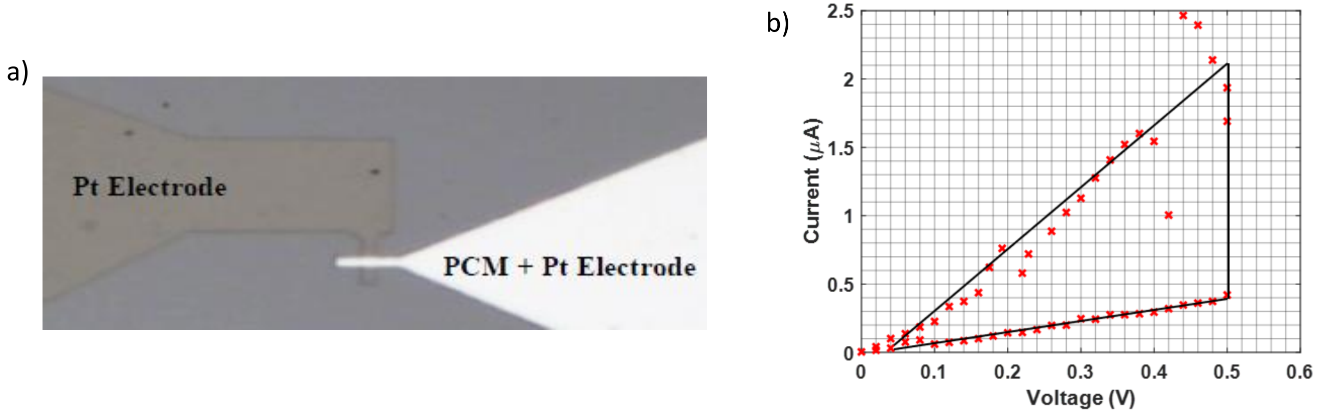

Figure 3. a) Optical microscope image of the cross region of a GST-725 crossbar device under x50 magnification. The cross region is of size 1.0 μm x 1.0 μm. b) I-V characteristic obtained for GST-725 crossbar device, starting in the amorphous phase (lines just a guide to the eye).

4. Device Modelling

To help further understand the functioning of PCMs for use in flexible electronics, simulations of the operation of memory devices which are suitable for integration into a flexible electronics architecture were carried out. To do this a model is used that combines thermoelectric finite-element simulations (using COMSOL Multiphysics) with a ‘bespoke’ phase-change model based on a Gillespie type cellular automata and classical nucleation and growth theory.[19-21] Finite-element simulations are used to model the Joule heating caused by the flow of current through the phase-change layer in a defined memory geometry when a voltage pulse is applied. These calculations are carried out using a coupled system of equations consisting of the Laplace equation (Equation 1) for the electric model and the heat diffusion equation (Equation 2) for the thermal model.[22]

$$\nabla\sigma \cdot \nabla V = 0 \qquad (1)$$

$$\rho C_p \frac{\partial T}{\partial t} - K \cdot \nabla^2 T = \sigma |E|^2 \qquad (2)$$

Here σ is the electrical conductivity,[22] V the electric potential, C_p, ρ and K are material parameters corresponding to the specific heat capacity, density, and thermal conductivity respectively. The resulting electric field and temperature distributions produced are used to

calculate crystal nucleation and growth rates for each point in a cellular grid of GST 'monomers' constructed throughout the phase-change layer and with spacing equal to the diameter of a single GST monomer (~0.82 nm).[21] In this model each monomer can be either amorphous or crystalline, single monomers can nucleate from the amorphous phase and then grow out into larger crystallites, crystallizing the monomers around them. The equations for nucleation and growth can be seen in Equation 3 and Equation 4 respectively.

$$I^{ss} = \left(\frac{4}{v_m}\right)\gamma n_c^{\frac{2}{3}}\sqrt{\frac{\Delta g}{6\pi K_B T n_c}}\exp\left(-\frac{\Delta G_c}{K_B T}\right) \quad (3)$$

$$V_g = \frac{4rK_BT}{3\pi\lambda_j{}^2 R_h \eta(T)}\left[1-\exp\left(-\frac{\Delta g}{K_BT}\right)\right] \quad (4)$$

Here, v_m is the volume of a monomer, n_c is the number of monomers in a critical cluster, Δg is the Gibbs free energy between the liquid and solid states per monomer, ΔG_c is the energy barrier for nucleation, r and R_h are the atomic radius and the hydrodynamic radius, λ the diffusional jump distance and $\eta(T)$ is the viscosity.[20] A list of parameters and their values is provided in **Table 1**, here v_m is the volume of a GST monomer, ΔH_f is the enthalpy of fusion at melting point, σ_i is the interfacial energy and T_m is the melting temperature. The joint nucleation and growth rates from the model are used to calculate the resulting crystalline distribution and crystal microstructure when a memory device is excited by an applied voltage pulse.

Table 1. Model parameters used in the simulation of GST-225 memory cells.

Parameter	Value	Parameter	Value
C_p	210 $Jkg^{-1}K^{-1}$ [22]	r	0.1365 x 10^{-9} m [20] [25]
ρ	6150 kgm^{-3} [22]	R_h	0.1365 x 10^{-9} m [20] [25]
K	Am: 0.2 $Wm^{-1}K^{-1}$ Cr: 0.58 $Wm^{-1}K^{-1}$ [22] [23]	λ	2.99 x 10^{-10} m [21]
n_c	$\mathbf{n_c} = \frac{32\pi}{3}\frac{v_m{}^2\sigma_i{}^3}{\Delta g^2}$ [21]	ΔH_f	625 x 10^6 Jm^{-3} [21]
Δg	$\frac{\Delta g}{v_m} = \frac{T_m - T}{T_m}\frac{2T}{T_m + T}$ [24]	σ_i	0.06 Jm^{-2} [20] [26]
ΔG_c	$\mathbf{\Delta G_c} = \frac{16\pi}{3}\frac{v_m{}^2\sigma_i{}^3}{\Delta g^2}$ [21]	T_m	900 K [21]
v_m	2.9 x 10^{-28} m^3 [21]		

To demonstrate the operation of the above model, and to give some assurance in terms of its outputs, we first explored the switching of the archetypal GST-225 composition whose

properties are perhaps best understood/documented. In **Figure 4**, for example, we show the simulated temperature dependence of the nucleation and growth mechanisms in a blanket film of GST-225 subject to a linear temperature gradient. Here we can see that at lower temperatures nucleation of small crystalline clusters dominates. When progressing to higher temperatures the growth mechanism is the main cause of crystallization, up until the melting temperature where any crystalline structure will melt. The temperatures for maximum nucleation rate and growth rate, and the maximum growth rate itself, match well to those eported in the literature.[27,28]

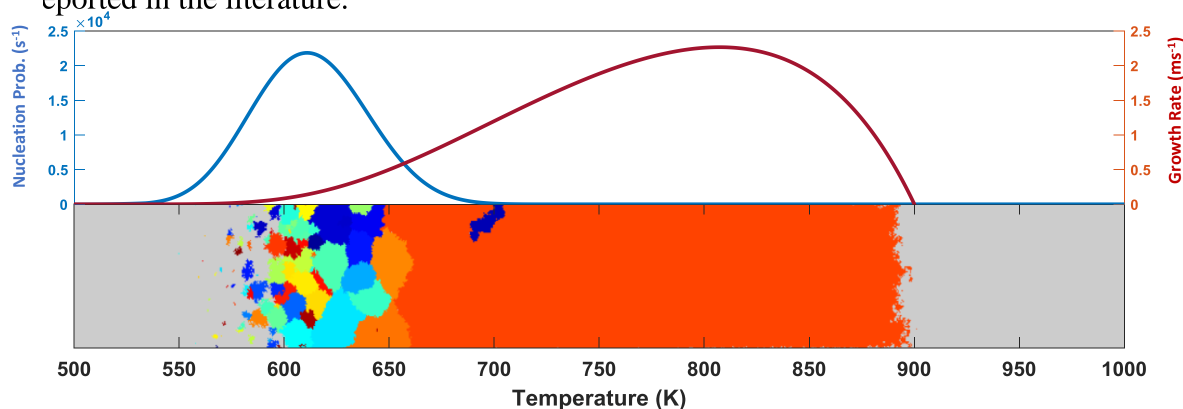

Figure 4. A simulation displaying the crystallization of a GST-225 blanket film subject to a temperature gradient (and after a time duration of 300 ns). Here, the grey areas are amorphous and the coloured regions represent crystallite grains of different orientations. The nucleation and growth rate are also plotted along the same temperature gradient to display the temperature dependence of the two processes and easily visualise the resulting crystal microstructure as a function of temperature.

Now that a suitable model for simulating phase switching in memory cells has been created, we model a pore-cell device which has the potential to be integrated into low-cost flexible electronics systems. Here, a flexible polyimide substrate and, initially, GST-225 is used as the phase-change layer. The detailed geometry of the device and simulated switching results can be seen in **Figure 5**. Firstly, an amorphous area is melted into the pore to leave the cell in the high resistance state. Then a 1.95 V, 5 µs pulse (with a fall time of 2 µs) is used to re-crystallize this amorphous region; this operation is successful and the device changes to a lower electrical resistance as there is now a conductive path of crystalline material connecting the electrodes. An attempt to reamorphize a device in the set state using a 3.0 V, 3 µs pulse (with a fall time of 200 ns) is made. Such relatively long pulse lengths are appropriate since

they are most likely achievable in low-cost and easy-to-mass-produce flexible electronic systems. However, such pulse lengths are significantly longer than those used in 'conventional' phase-change memories and, unsurprisingly, lead in this case to, significant recrystallization of the melted area occurring during the attempted amorphization process. We see therefore that the device remains in a low resistance state, since a conductive path of crystalline material is connecting the electrodes. This shows that phase-change materials which operate on the speeds such as those seen in GST-225 have the potential to undergo unwanted recrystallization in the reamorphization step, and that this is facilitated by the longer pulse times typically used in flexible electronic systems. This issue will also apply to GST-725 which is considered to have a very similar crystallization speed to GST-225.[29] However, the simulation results of Figure 5, taken along with the experimental GST-725 switching results shown in Figure 3 (and as reported in the literature by others [10,12,30]), do point the way to the realization of a simple write-once memory suitable for use with flexible electronics using Ge-rich materials such as GST-725. Such materials can, due to their high crystallization temperature, maintain their amorphous phase during manufacture. Their crystallization in pore-type cells suited to give a write-once functionality in flexible device applications should then be straightforward. Of course, it would be preferable to have a fully re-writable memory suited to flexibles, and to achieve this aim we now explore the use of slow crystallization materials that should be easier to reamorphize with switching pulses suited to low-cost flexible electronics implementations.

One potentially suitable slow crystallization material to enable the provision of a fully rewritable memory of use in low-cost flexible electronics is Se-substituted GST, such as $Ge_2Sb_2Se_4Te$ (GSST-2241). Alongside a slower crystal growth rate, GSST-2241 still offers an increased crystallization temperature (T_C) compared to GST-225, as previously reported [31] and as shown in this paper in Figure 1 where a T_C of ~305ºC is seen. The successful reamorphization of GSST-2241 has also been previously demonstrated using relatively long excitation pulses, at least in photonic applications using embedded microheaters.[32]

To test whether the slower crystallization properties of GSST-2241 prevent unwanted recrystallization during the relatively long-lived reamorphization operation likely to be used in flexible devices, we carry out device switching simulations similar to those shown previously for GST-225 in Figure 5. However, different material parameters for GSST-2241 are obviously required to be used in the simulation model. These were extracted from

previously published reports where available, and consisted of new thermal conductivity data,[33] melting temperature,[11] activation energy for crystallization[34] and crystallization temperature.[14] Alongside this, viscosity and growth rate values more suited to GSST-2241 were used,[11]

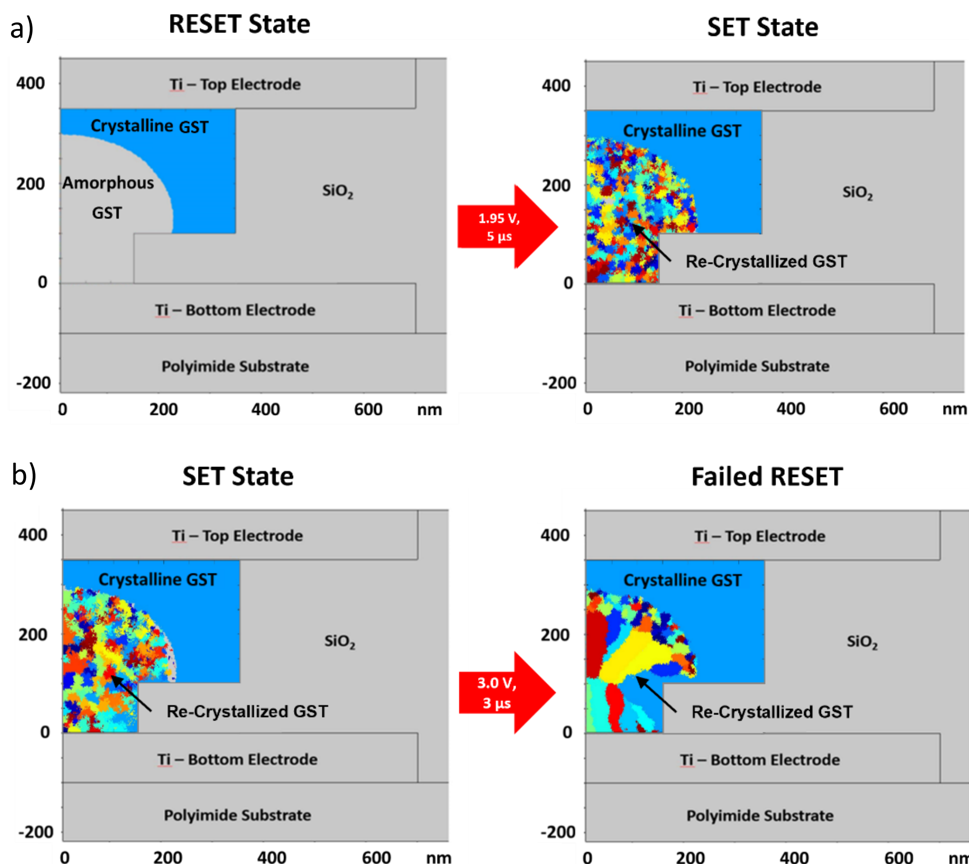

Figure 5. a) Simulation of the switching of a GST-225 pore memory cell from the amorphous state to the crystalline state using a 1.95 V, 5 μs pulse (fall time 2 μs). b) Simulation of an attempt to reamorphize the memory cell via the application of a 3.0 V, 3 μs pulse (fall time 200 ns). The cell resistance in the initial RESET state was 72.1 kΩ, in the SET state it was 1.56 kΩ and in the failed RESET state it was 1.55 kΩ. Note that the simulations here are 2D (and assumed radially symmetric), and the device schematic shows half the simulation space with the y-axis being the centre line of the device.

resulting in a maximum simulated growth rate for GSST-2241 in our model of 1.7×10^{-3} ms^{-1}, compared to the conventionally accepted maximum GST-225 growth rate of ~3 ms^{-1}.[27] **Table 2** provides a summary of the new material parameters used to model GSST-2241.

To demonstrate the slower crystal growth speed of GSST-2241 in our model, simulations of a 100 nm x 100 nm area of phase-change material cooling from above the material melting temperature at various rates were carried out and compared to those predicted for GST-225. The resulting phase distributions once the material has cooled to room temperature are displayed in **Figure 6**. It can clearly be seen that far more rapid cooling rates are required for GST-225 to remain in the amorphous phase compared to GSST-2241.

Table 2. Model parameters used in the simulation of GSST-2241 memory cells.

Parameter	Value	Parameter	Value
C_p	285 $Jkg^{-1}K^{-1}$ [33]	R_h	0.125 x 10^{-9} m [35]
ρ	5270 kgm^{-3} [33]	λ	2.60 x 10^{-10} m [35]
K	Am: 0.2 $Wm^{-1}K^{-1}$ Cr: 0.48 $Wm^{-1}K^{-1}$ [33]	ΔH_f	625 x 10^{6} Jm^{-3} [21]
ν_m	2.62 x 10^{-28} m^3 [33]	σ_i	0.038 Jm^{-2} [36]
r	0.125 x 10^{-9} m [35]	T_m	793 K [34]

Having confirmed the slower crystallization speed of GSST-2241 is captured by our crystallization modelling, simulations of switching of GSST-2241 in the same pore cell structure used previously in Figure 5 were carried out. The results are seen in **Figure 7**. As before, initially an amorphous area is melted into the pore, then a 2.0 V, 14 μs (fall time 1 μs) pulse is used to recrystallize the cell. Following this a 3.0 V, 3 μs pulse (fall time 200 ns) is used to attempt to reamorphize the device. Unlike in the GST-225 case, this reamorphization is successful, due to the significantly reduced crystal growth speed of GSST-2241. A high cell resistance is recovered, and there is no evidence of a path of conductive material connecting the electrodes. Here we have demonstrated that using GSST-2241 we can simulate a fully re-writable memory cell with long reset pulses that are suitable for use in low-cost flexible electronic systems.

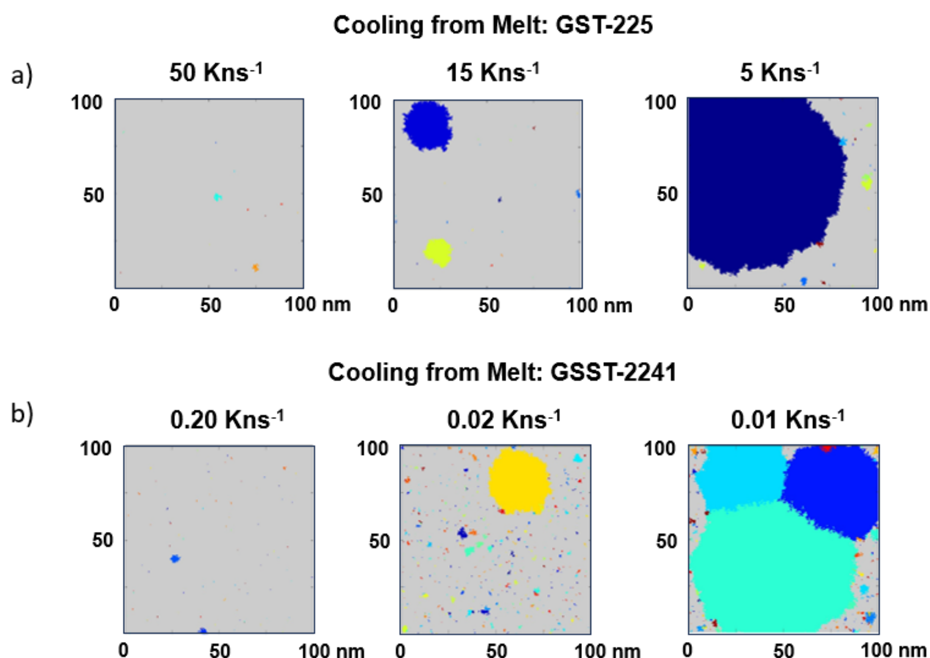

Figure 6. a) Simulation of a 100 nm x 100 nm square of GST-225 being cooled from above melting temperature to room temperature at rates 50 Kns^{-1}, 15 Kns^{-1} and 5 Kns^{-1}. Here significant recrystallization upon cooling is observed for cooling rates slower than 15 Kns^{-1}. b) Simulation of a 100 nm x 100 nm square of GSST-2241 being cooled from above melting temperature to room temperature at rates 0.2 Kns^{-1}, 0.02 Kns^{-1} and 0.01 Kns^{-1}. For this material significantly slower cooling rates can exist before recrystallization is observed. In both figures grey areas are amorphous and the different coloured regions represent different crystallite grain orientations.

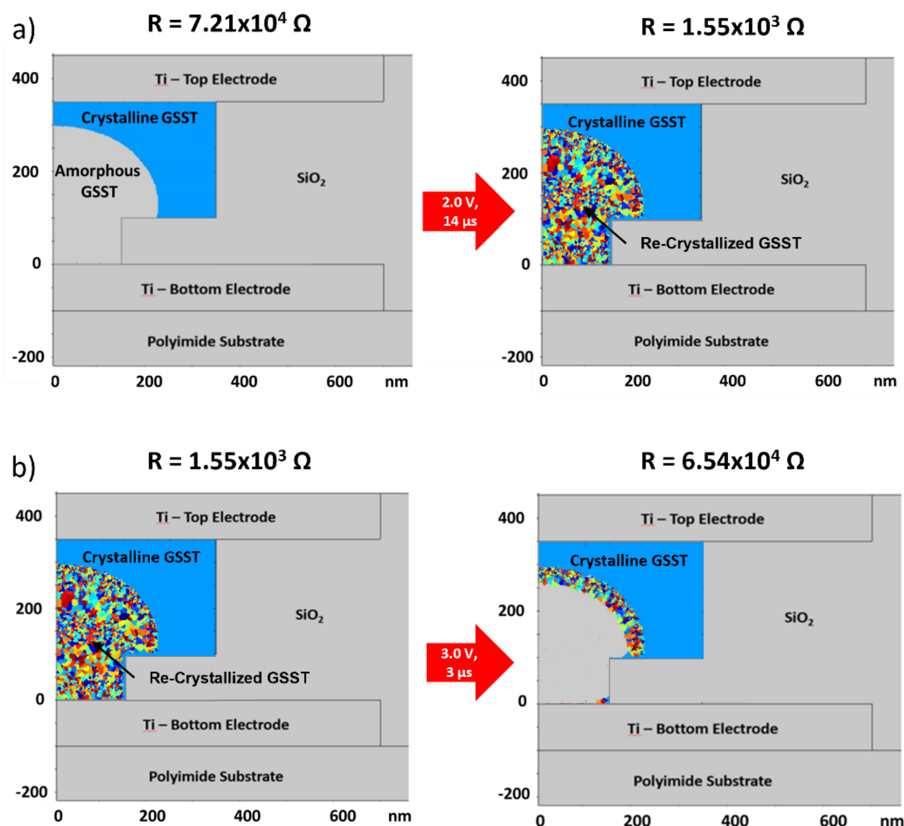

Figure 7. a) Simulation of the switching of a pore memory cell using GSST-2241 material from the amorphous state to the crystalline state using a 2.0 V, 14 µs pulse. b) Simulation of the reamorphization of the memory cell using a 3.0 V, 3 µs pulse. No significant recrystallization is observed, despite the extended length of the pulse, due to the slow crystallization speed of GSST-2241. Cell resistance is calculated for each crystalline distribution. Note that the simulations here are 2D (and assumed radially symmetric), and the device schematic shows half the simulation space with the y-axis being the centre line of the device.

6. Conclusion

The high temperature crystallization properties of the materials GST-725, GST-825 and GSST-2241 were successfully characterized through in-situ measurement of electrical resistivity. Such materials are useful for improving data retention properties of phase-change memories at elevated temperatures and importantly can allow for retention of the amorphous phase during high temperature manufacturing processes, in turn facilitating the simple implementation of write-once memories for flexible electronics applications. Indeed, write-once switching of GST-725 devices in a crossbar configuration was successfully

demonstrated. Simulations using a joint finite-element electrothermal and Gillespie Cellular Automata phase-change modelling approach were used to explore the switching of phase-change memories on flexible Polyimide substrates. GST-225 was successfully crystallized in a pore-cell device suitable for flexible electronics applications. However, there were issues with the reamorphization step when using the relatively long excitation pulses - on the order of μs - typically available in low-cost flexible electronic systems. Indeed, for GST-225 significant crystallization was seen when trying to reamorphize pore cell type devices designed for use in flexible systems, precluding the realization of a rewritable memory. As a solution to this problem, the use of GSST-2241 was proposed as this has a much slower crystal growth rate as compared to GST-225. Our crystallization model was updated to include material parameters relevant to GSST-2241, and simulations of the same pore cell devices showed that the slow growth rate suppressed significant recrystallization during the amorphization step, demonstrating, at least in simulation, a fully rewritable memory suitable for use in flexible electronics implementations.

Acknowledgements
CDW and JP acknowledge financial support for this work from the UK EPSRC via grant number EP/L015331/1. JP also gratefully acknowledges financial support from PragmatIC Semiconductor Ltd.

Rights Statement
For the purpose of open access, the author has applied a Creative Commons Attribution (CC BY) licence to any Author Accepted Manuscript version arising from this submission

Received: ((will be filled in by the editorial staff))
Revised: ((will be filled in by the editorial staff))
Published online: ((will be filled in by the editorial staff))

References

[1] S. Kumar, P. Tiwari, M. Zymbler, *Journal of Big Data*. **2019**, 6, 111, https://doi.org/10.1186/s40537-019-0268-2

[2] Y. Gu, T. Zhang, H. Chen, F. Wang, Y. Pu, C. Gao, S. Li. Nanoscale Res. Lett. **2019**, 14, 263, https://doi.org/10.1186/s11671-019-3084-x

[3] S. F. Wamba, A. Anand, L. Carter. Procedia Technology. **2013**, 9, 421, https://doi.org/10.1016/j.protcy.2013.12.047

[4] M. L. Gallo, A. Sebastian, *J. Phys. D: Appl. Phys.* **2020**, 53, 213002, https://doi.org/10.1088/1361-6463/ab7794

[5] W. J. Wang, L. P. Shi, R. Zhao, K. G. Lim, H. K. Lee, T. C. Chong, Y. H. Wu, *Appl. Phys. Lett.* **2008,** 93, 043121, https://doi.org/10.1063/1.2963196

[6] D. Deleruyelle, M. Putero, T. Ouled-Khachroum, M. Bocquet, M.-V. Coulet, X. Boddaert, C. Calmes, C. Muller, *Solid-State Electron.* **2013**, 79, 159-165, https://doi.org/10.1016/j.sse.2012.06.010

[7] A. I. Khan, A. Daus, R. Islam, K. M. Neilson, H. R. Lee, H.-S. P. Wong, E. Pop, *Science* **2021,** 373, 1243-1247, https://doi.org/10.1126/science.abj1261

[8] P, Zuliani, E. Varesi, E. Palumbo, M. Borghi, I. Tortorelli, D. Erbetta, G. D. Libera, N. Pessina, A. Gandolfo, C. Prelini, L. Ravazzi, R. Annunziata, *IEEE Trans. Electron Devices,* **2013**, 60, 12, 4020-4026, https://doi.org/10.1109/TED.2013.2285403

[9] S. Cecchi, I. L. Garcia, A. M. Mio, E. Zallo, O. A. El Kheir, R. Calarco, M. Bernasconi, G. Nicotra, S. M. S. Privitera, *Nanomaterials* **2022**, 12**,** 631, https://doi.org/10.3390/nano12040631

[10] S. M. S. Privitera, I. L. García, C. Bongiorno, V. Sousa, M. C. Cyrille, G. Navarro, C. Sabbione, E. Carria, E. Rimini, *J. Appl. Phys.* **2020**, 128, 155105, https://doi.org/10.1063/5.0023696

[11] J. Bartak, P. Kostal, J. Malek, *J. Non-Cryst. Solids* **2019**, 505 1–8, https://doi.org/10.1016/j.jnoncrysol.2018.10.048

[12] S. M. S. Privitera, S. Cecchi, I. L. Garcia, A. M. Mio, M. C. Cyrille, N-P. Tran, G. D'Arrigo, in *Proc. European Phase Change and Ovonics Symposium (E\PCOS),* Sapienza Università di Roma, Rome, **2023**, 62

[13] Y. Zhang, J. B. Chou, J. Li, H. Li, Q. Du, A. Yadav, S. Zhou, M. Y. Shalaginov, Z. Fang, H. Zhong, C. Roberts, P. Robinson, B. Bohlin, C. Ríos, H. Lin, M. Kang, T. Gu, J.

Warne, V. Liberman, K. Richardson, J. Hu, *Nat. Commun.* **2019**, 10, 4279, https://doi.org/10.1038/s41467-019-12196-4

[14] A. A. Burtsev, N. N. Eliseev, V. A. Mikhalevsky, A. V. Kiselev, V. V. Ionin, V. V. Grebenev, D. N. Karimov, A. A. Lotin, *Mater. Sci. Semicond. Process.,* **2022**, 150, 106907*,* https://doi.org/10.1016/j.mssp.2022.106907

[15] E. Petroni, A. Serafini, D. Codegoni, P. Targa, L. Mariani, M. Scuderi, G. Nicotra, A. Redaelli*, Front. Phys.* **2022**, 10:862954, https://doi.org/10.3389/fphy.2022.862954

[16] E. Rahier, M. Luong, S. Ran, N. Ratel-Ramond, S. Saha, C. Mocuta, D. Benoit, Y. Le-Friec, A. Claverie, *Phys. Status Solidi RRL*, **2023**, 17, 2200450. https://doi.org/10.1002/pssr.202200450

[17] M. Agati, M. Vallet, S. Joulié, D. Benoit, A. Claverie, *Mater. Chem. C.* **2019**, 7, 8720,

[18] YY. Au, H. Bhaskaran, C. D. Wright, *Sci. Rep.* **2017,** 7, 9688 https://doi.org/10.1038/s41598-017-10425-8

[19] P. Ashwin, B. S. V. Patnaik, C. D. Wright, *J. Appl. Phys.* **2008**, 104, 084901, https://doi.org/10.1063/1.2978334

[20] Y. Wang, J. Ning, L. Lu, M. Bosman, R. E. Simpson, *npj Comput. Mater.,* **2021**, 7, 183, https://doi.org/10.1038/s41524-021-00655-w

[21] S. Senkader, C. D. Wright, *J. Appl. Phys.* **2004**, 95, 504, https://doi.org/10.1063/1.1633984

[22] C. D. Wright, M. Armand, M. M. Aziz, *IEEE Trans. Nanotechnol.* **2006**, 5, 1, 50, https://doi.org/10.1109/TNANO.2005.861400

[23] H-K. Lyeo, D. G. Cahill, B-S. Lee, J. R. Abelson, M-H. Kwon, K-B. Kim, S. G. Bishop, B-k. Cheong, *Appl. Phys. Lett.* **2006**, 89, 15, 151904, https://doi.org/10.1063/1.2359354

[24] C. V. Thompson, F. Spaepen, *Acta Metall.* **1979**, 27, 12, 1855-1859, https://doi.org/10.1016/0001-6160(79)90076-2

[25] A. Sebastian, M. Le Gallo, D. Krebs, *Nat. Commun.* **2014**, 5, 4314, https://doi.org/10.1038/ncomms5314

[26] H. Attariani, W. Wang, R. Gałek, *J. Cryst. Growth,* **2020**, 542, 125687, https://doi.org/10.1016/j.jcrysgro.2020.125687

[27] J. Orava, A. L. Greer, B. Gholipour, D. W. Hewak, C. E. Smith, *Nature Mater.* **2012**, 11, 279, https://doi.org/10.1038/nmat3275

[28] J. Orava, A. L. Greer, *Acta Mater.* **2017**, 139, 226, https://doi.org/10.1016/j.actamat.2017.08.013

[29] M. Baldo, L. Laurin, E. Petroni, G. Samanni, M. Allegra, E. Gomiero, D. Ielmini, A. Redaelli, *2022 IEEE International Memory Workshop (IMW)*, **2022**, 1, https://doi.org/10.1109/IMW52921.2022.9779290

[30] A. D. Fattorini, C. Chèze, I. L. García, C. Petrucci, M. Bertelli, F. R. Riva, S. Prili, S. M. S. Privitera, M. Buscema, A. Sciuto, S. Di Franco, G. D'Arrigo, M. Longo, S. De Simone, V. Mussi, E. Placidi, M. Cyrille, N-P. Tran, R. Calarco, F. Arciprete, *Nanomaterials* **2022**, 12, 8, 1340, https://doi.org/10.3390%2Fnano12081340

[31] H. Wang, T, Guo, Y. Xue, S. Lv, D. Yao, Z. Zhou, S. Song, Z. Song, *Mater. Lett.* **2019**, 254, 182, https://doi.org/10.1016/j.matlet.2019.07.031

[32] Y. Zhang, C. Fowler, J. Liang, B, Azhar1, M. Y. Shalaginov, S. Deckoff-Jones, S. An, J. B. Chou, C. M. Roberts, V. Liberman, M. Kang, C. Ríos, K. A. Richardson, C. Rivero-Baleine, T. Gu, H. Zhang, J. Hu, *Nat. Nanotechnol.* **2021**, 16, 661, /https://doi.org/10.1038/s41565-021-00881-9

[33] K. Aryana, Y. Zhang, J. A. Tomko, Md. S. B. Hoque, E. R. Hoglund, D. H. Olson, J. Nag, J. C. Read, C. Ríos, J. Hu, P. E. Hopkins, *Nat. Commun.,* **2021**, 12, 7187, https://doi.org/10.1038/s41467-021-27121-x

[34] R. Svoboda, J. Malek, *J. Alloys Compd.,* **2015**, 627, 287, https://doi.org/10.1016/j.jallcom.2014.12.007

[35] H. Zhang, X. Wang, W. Zhang, *Opt. Mater. Express* **2022**, 12, 7, 2497-2506, https://doi.org/10.1364/OME.462846

[36] Tomáš Halenkovič, M. Baillieul, J. Gutwirth, Petr Němec, V. Nazabal, *J. Mater.* **2022**, 8, 5, 1009-1019, https://doi.org/10.1016/j.jmat.2022.02.013

Table of Contents

Flexible Electronics Applications of Ge-rich and Se-Substituted Phase-change Materials in Non-volatile Memories

J. Pady, J. Costa, C. Ramsdale, F. Alkhalil, A. Nevill, M. F. Craciun, C. D. Wright*

Flexible electronics that are easy to manufacture and integrate into everyday items require suitable non-volatile memory technology. Here we explore Ge-rich GeSbTe and Se-substituted GeSbSeTe phase-change alloys for such applications. Key material properties are measured using 4-point probe electrical testing, Raman spectroscopy and X-ray diffraction. Devices suited to both write-once and re-writable memory implementations are also investigated, through both simulation and experiment.